**da Costa Filho, Carlos Alberto and Tant, Katherine and Curtis, Andrew and Mulholland, Anthony and Moran, Carmel M. (2018) Using laboratory experiments to develop and test new Marchenko and imaging methods. In: SEG Technical Program. Society of Exploration Geophysicists, Tulsa, OK., pp. 4352-4356. , http://dx.doi.org/10.1190/segam2018-2979521.1**

# Using laboratory experiments to develop and test new Marchenko and imaging methods

*Carlos Alberto da Costa Filho (University of Edinburgh), Katherine Tant (University of Strathclyde), Andrew Curtis* (University of Edinburgh), Anthony Mulholland (University of Strathclyde) and Carmel M. Moran (University of Edinburgh)*

## SUMMARY

The Marchenko redatuming method estimates surface-to-subsurface Green's functions. It has been employed to diminish the effects of multiples in seismic data. Several such methods rely on an absolute scaling of the data; this is usually considered to be known in synthetic experiments, or is estimated using heuristic methods in real data. Here, we show using real ultrasonic laboratory data that the most common of these methods may be ill suited to the task, and that reliable ways to estimate scaling remains unavailable. Marchenko methods which rely on adaptive subtraction may therefore be more appropriate. We present two adaptive Marchenko methods: one is an extension of a current adaptive method, and the other is an adaptive implementation of a non-adaptive method. Our results show that Marchenko methods improve imaging compared to reverse-time migration, but less so than expected. This reveals that some Marchenko assumptions were violated in our experiment and likely are also in seismic data, showing that laboratory experiments contribute critical information to the development and testing of Marchenko-based methods.

## INTRODUCTION

Seismic processors have long been concerned with the presence of multiples (waves that reflect multiple times in the subsurface before being recorded at the receiver array) in seismic data. Many methods have been devised to either remove (Verschuur, 1992; Araújo et al., 1994; Fokkema et al., 1994; Weglein et al., 1997; Ziolkowski et al., 1999; Amundsen, 2001), incorporate (Reiter et al., 1991; Youn and Zhou, 2001; Brown and Guitton, 2005; Jiang et al., 2005; Berkhout and Verschuur, 2006; Malcolm et al., 2009; Liu et al., 2011; Fleury, 2013; Zuberi and Alkhalifah, 2014) or otherwise bypass the presence of multiples in the data (Meles et al., 2016). Nevertheless, a method to process multiples which supplants all others remains elusive.

The most recent additions to the family of multiple-processing tools are those stemming from the Marchenko method (Rose, 2001; Broggini et al., 2012; Wapenaar et al., 2013). The Marchenko method purports to construct full surface-to-subsurface Green's functions (i.e. including multiples) with only limited knowledge of the subsurface (namely, a migration velocity macro-model), and the reflection response.

Beyond receiver redatuming, the Marchenko method has also been applied to migration-style imaging (Broggini et al., 2014; Wapenaar et al., 2014), source and receiver redatuming (Wapenaar et al., 2014; van der Neut and Wapenaar, 2016; Vasconcelos et al., 2017), internal multiple attenuation (Meles et al., 2014; da Costa Filho et al., 2017), primary estimation (Meles et al., 2016), and subsurface wavefield retrieval (Wapenaar et al., 2016; Singh and Snieder, 2017).

Few works, however, consider field or lab data, and consequently most fail to demonstrate their validity in a practical setting. While this may not be an issue for tried-and-tested methods about the data such as reverse-time migration (RTM), it is crucial for an incipient method such as the Marchenko method. This importance is highlighted by the fact that a large subset of Marchenko-based methods require unrealistic assumptions such as broadband, wide coverage, densely sampled, multicomponent data whose amplitude should be normalized to an (a priori unknown) scaling factor.

In this work, we test and improve two Marchenko-based methods using a real laboratory ultrasonic dataset, and show that while they may offer some improvements over traditional methods, these improvements tend to be much more modest than results shown for synthetic experiments. We thus demonstrate how controlled laboratory experiments contribute to the practical development of new imaging methods.

## METHODOLOGY

The Marchenko method constructs up- and downgoing surface-to-subsurface Green's functions from the reflection response and so-called focusing functions through the following discretized equations (van der Neut et al., 2015b)

$$\mathbf{g}^- = -\mathbf{f}^- + \mathbf{R}\mathbf{f}^+ \tag{1}$$

$$\mathbf{Z}\mathbf{g}^+ = \mathbf{f}^+ - \mathbf{R}\mathbf{Z}\mathbf{f}^- \tag{2}$$

where $\mathbf{g}^-$ and $\mathbf{g}^+$ represent the up- and downgoing Green's functions, written as time-domain gathers concatenated in time to form vectors; $\mathbf{f}^-$ and $\mathbf{f}^+$ represent the up- and downgoing focusing functions in similar vector format; operator $\mathbf{R}$ represents multidimensional convolution with the reflection response; and $\mathbf{Z}$ is the time reversal operator. To obtain $\mathbf{g}^\pm$ from these equations, one must first estimate the focusing functions $\mathbf{f}^\pm$. This can achieved through an iterative approach (Broggini et al., 2012; Wapenaar et al., 2014) or inversion (van der Neut et al., 2015a; Ravasi, 2017).

Regardless of the method, Marchenko theory requires the reflection response to be scaled to a particular magnitude, namely, it must be twice the vertical velocity response from a negative pressure impulsive point source. In reality, the measured reflection response is, at best, a scaled version of this ideal reflection response. $\mathbf{R}$ in equations 1 and 2 is commonly substituted for a scaled convolution with the measured reflection response, denoted by $a\widetilde{\mathbf{R}}$.

Few methods exist to estimate scaling factor $a$. Thomsen (2016) requires vertical seismic profile (VSP) data, which is impractical in many scenarios. In the first application of the

Marchenko method to real data, Ravasi et al. (2016) analyze the convergence of the iterative scheme to hand-pick a value. van der Neut et al. (2015b), Brackenhoff (2016) and Mildner et al. (2017) provide a more automated approach consisting of minimizing costs functions which depend only on the surface reflection data. We follow van der Neut et al. (2015b) who use

$$j(a) = \frac{\|\mathbf{g}^-\|_2}{\|\mathbf{g}_0^-\|_2} \tag{3}$$

where $\mathbf{g}_0^- = (\mathbf{I}-\mathbf{M})a\widetilde{\mathbf{R}}\mathbf{f}_d^+$ is the first Marchenko iteration of the final constructed upgoing field, $\mathbf{g}^-$, $\|\cdot\|_2$ is the $L^2$ vector norm, $\mathbf{I}$ is the identity, $\mathbf{M}$ is a matrix which mutes arrivals after direct wave and before its time reverse, and $\mathbf{f}_d^+$ is the initial estimate of the focusing function (e.g. a time-reversed direct wave). It is important to note that both $\mathbf{g}_0^-$ and $\mathbf{g}^-$ depend on the scaling $a$.

The approximate effect of the Marchenko iteration on $\mathbf{g}^-$ is to remove multiple energy from the standard estimate $\mathbf{g}_0^-$. This should happen when $j(a)$ is minimized. However, as our numerical results will show, this curve may not always have a reasonable minimum in practice. In such cases, the vast majority of Marchenko methods which require knowledge of the scaling will not be applicable. We therefore analyze and extend two methods which have been designed to use real data with an unknown scaling factor.

The first is an adaptive imaging method based on van der Neut et al. (2014), where the iterative solution to equations 1 and 2 is truncated at iteration 2, and the update is added adaptively:

$$\mathbf{g}^- \approx \mathbf{g}_0^- + \alpha * \mathbf{g}_\Delta^- \tag{4}$$

where $\alpha$ is a short filter, $*$ is convolution and

$$\mathbf{g}_\Delta^- = (\mathbf{I}-\mathbf{M})\widetilde{\mathbf{R}}\mathbf{Z}\mathbf{M}\widetilde{\mathbf{R}}\mathbf{Z}\mathbf{M}\widetilde{\mathbf{R}}\mathbf{f}_d^+. \tag{5}$$

The imaging condition at a certain location $\mathbf{x}$ is then given by

$$I_{\mathrm{aMI}}(\mathbf{x}) = \sum \mathbf{g}_0^+ \circ \mathbf{g}^- \tag{6}$$

where $\circ$ represents element-wise multiplication between the two vectors. For comparison, standard RTM is equivalent to

$$I_{\mathrm{RTM}}(\mathbf{x}) = \sum \mathbf{g}_0^+ \circ \mathbf{g}_0^-. \tag{7}$$

We modify this method by enhancing the adaptive subtraction. First, instead of a simple convolution operator, we use regularized nonstationary regression (Fomel, 2009). In addition, we know that the image is constructed from events in $\mathbf{g}^-$ which intersect in time and space with $\mathbf{g}_0^+$. Therefore, it stands to reason that we limit the computation of the adaptive filter as well as the image to include only events near the direct wave. Finally, we also "flatten" the $\mathbf{g}_0^-$ and $\mathbf{g}_\Delta^-$ gathers by subtracting trace by trace the traveltime of the direct wave. This procedure is akin to a standard normal moveout (NMO) correction, although it does not suffer from the characteristic NMO stretching nor is it limited to hyperbolic moveouts. Of course, this procedure does not fully flatten the upgoing gathers, but it does considerably diminish the dips of events, ensuring higher lateral continuity and thus improving the adaptive filter. The new imaging condition becomes

$$I_{\mathrm{AMI}}(\mathbf{x}) = \sum \mathbf{g}_0^+ \circ \mathbf{g}_w^- \tag{8}$$

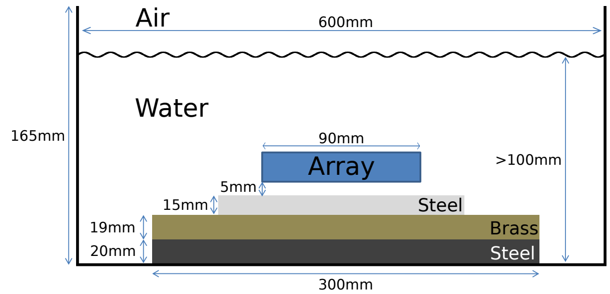


Figure 1: Laboratory setup for ultrasonic acquisition. We measured the velocities in plates as 6465 m/s, 4388 m/s, 5926 m/s respectively from top to bottom. Dimensions are not to scale.

where

$$\mathbf{g}_w^- = \mathbf{W}\mathbf{g}_0^- + \mathbf{S}^{-1}\hat{\mathbf{A}}\mathbf{S}\mathbf{W}\mathbf{g}_\Delta^- \tag{9}$$

where $\mathbf{W}$ mutes the data, $\mathbf{S}$ is the time-shifting operator, and $\hat{\mathbf{A}}$ is the nonstationary regression matching $\mathbf{S}\mathbf{W}\mathbf{g}_0^-$ to $\mathbf{S}\mathbf{W}\mathbf{g}_\Delta^-$.

In addition to imaging, another Marchenko method exists which solely uses $\mathbf{g}^-$, and can benefit from our adaptive estimate $\mathbf{g}_w^-$. Meles et al. (2016) use the upgoing field $\mathbf{g}^-$ and the direct wave $\mathbf{g}_0^+$ to estimate prestack primaries $P$ by

$$P(\mathbf{x}_r, \mathbf{x}_s, t) \approx \sum_i \int_{S_i} \mathbf{g}_0^+(\mathbf{x}, \mathbf{x}_r, t) * \mathbf{g}_f^-(\mathbf{x}, \mathbf{x}_s, t) + \mathbf{g}_f^-(\mathbf{x}, \mathbf{x}_r, t) * \mathbf{g}_0^+(\mathbf{x}, \mathbf{x}_s, t)\, \mathrm{d}S_i \tag{10}$$

where $\mathbf{g}_f^-$ is the first event of $\mathbf{g}^-$, $\mathbf{x}$ represents virtual receivers along subsurface boundary $S_i$, $\mathbf{x}_r$ and $\mathbf{x}_s$ are on the acquisition surface, and the outer sum is performed along all subsurface boundaries of interest. This constructs primary arrivals reflected from the first interfaces below each boundary $S_i$.

When using real data, picking $\mathbf{g}_f^-$ from an inexact $\mathbf{g}^-$ may be unreliable, and thus we propose using $\mathbf{g}_w^-$ as a picking guide. This ensures that spurious arrivals before the primary are not picked by mistake. Moreover, $P$ can both provide an image free of adaptive-subtraction-related artifacts which may occur when using equations 6 or 8, and enhance other processing steps such as velocity analysis (Dokter et al., 2017).

## LABORATORY EXAMPLE

We tested the methods described above on an ultrasonic dataset obtained from a submerged laboratory acquisition depicted in Figure 1. The water column was deep enough so that several orders of internal multiples are recorded before the onset of the water-air reflection. The inspection was performed with a 128 element linear array (Vermon, France) (2.25 MHz central frequency and array element spacing of 0.7 mm) attached to a Dynaray® controller (Zetec, Canada) operating at a sampling rate of 100 MHz.

Figure 2 shows a central common shot gather before and after processing, which consisted of deconvolution, 3D-to-2D correction, $f$-$k$ filtering, and muting of surface waves and near-surface effects.

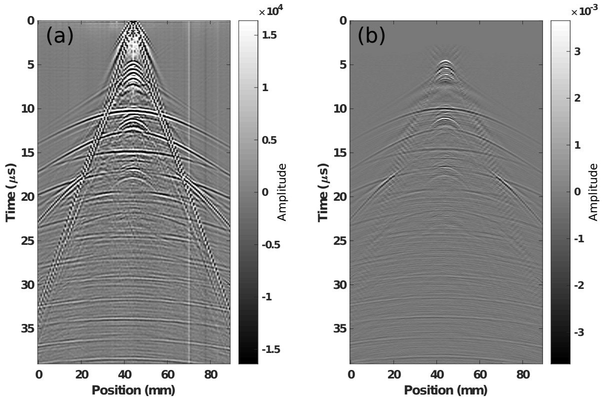


Figure 2: Common shot gather of (a) raw and (b) processed data.

We then attempted to obtain scaling factor $a$ for the data using the $j$-curve analysis of equation 3. Throughout, we use the velocity model in Figure 4 to compute all Green's functions and perform migration. Its horizontal extension coincides with that of the array. Vertically, however, we extend it much further than the physical dimensions of the setup, in order to capture internal multiples in the images.

The minimum of the $j$-curve is found by a one-dimensional bounded golden-section search. Unfortunately, as opposed to previous examples, the curve fails to have a reasonable minimum as shown in Figure 3. By inspection we observe that when using $a_{\min}$, the updates to $\mathbf{g}_0^-$ are negligible (i.e. $\|\mathbf{g}^- - \mathbf{g}_0^-\|_2 \approx 0$), which is seen from the fact that $j(a_{\min}) \approx 1$.

After verifying that this dataset may be inappropriate for standard Marchenko methods, we apply our adaptive Marchenko imaging based on equation 8 and compare it to standard RTM. The respective images can be found in Figures 5b and 5a. We observe two strong interfaces in both images corresponding to the depths of reflectors depicted in the schematic shown in Figure 1. The third interface should appear around 39 mm, but here the two images disagree. The RTM image shows a weak event at 39 mm which does not exist in the adaptive Marchenko image. A slightly stronger event appears around 35 mm and is indicated by the bottom-most white arrow in both images. Therefore, since the two earliest primaries appear slightly shifted upwards because of measurement, acquisition and velocity model inaccuracies, it seems most plausible that this stronger event represents the third interface.

The RTM image also exhibits several artifacts, some of which are indicated by black and red arrows. Many are attenuated in the adaptive Marchenko image, including the ones shown by the black arrows. Some others have remained almost untouched by adaptive Marchenko, as shown by red arrows.

Next, we applied the primary construction method using adaptive Marchenko guides. We show in Figure 5c the result of migrating this primaries-only dataset using RTM. The result shows perfect reconstruction of the first two reflectors and, if our interpretation is correct, of the third reflector as well. None

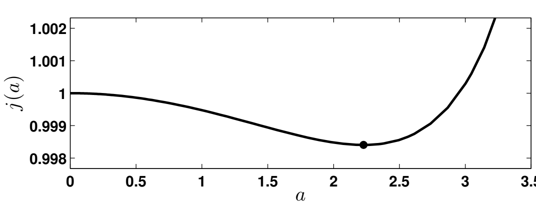


Figure 3: $j$-curve analysis of dataset. It attains its minimum $\min j(a) = 0.998$ at $a_{\min} = 2.237$ as shown by the black dot.

of the minor or major artifacts of RTM or adaptive Marchenko imaging appear in this image.

## DISCUSSION

The laboratory experiment was specifically designed to test the Marchenko method on real data in a controlled environment with known subsurface. We chose a simple layer cake model, used a submerged acquisition to remove surface-related reflections and attenuate elastic effects, and provided a densely sampled, fixed-spread acquisition. On the other hand, we remained ignorant of the source wavelet and scaling of the dataset.

The $j$-curve analysis provided little insight into this scaling factor, despite having apparently been successful in previous synthetic and field examples (van der Neut et al., 2015b; Brackenhoff, 2016; Mildner et al., 2017). We posit that this may be because of strong residual S-wave content which can be observed in Figure 2. Slight changes to this scheme such as changing norm to $L^1$ or omitting deconvolution does not improve the estimate. Therefore, it seems that in some such situations, an automated way of obtaining a reliable scaling factor may be beyond current technology.

The adaptive Marchenko image shows some improvements over standard RTM, as shown in Figure 5. This is expected given previous Marchenko imaging results (adaptive or non-adaptive). However, contrary to previous results, the improvement is lackluster, especially considering that the medium comprises horizontal layers whose velocities are known a priori. Indeed, the ideal Marchenko image would show only the three true reflectors, similarly to the image shown in Figure 5c. Again, a possible explanation for this may be the fairly strong S-wave content of the dataset. In a similar synthetic experiment, da Costa Filho et al. (2015) showed that S-waves create strong artifacts in acoustic Marchenko imaging of elastic media.

The best result is seen in Figure 5c, which shows the result of the adaptive-Marchenko-guided primaries-only imaging. However, this result has also been the most expensive to obtain because it involved manual picking of the events in $\mathbf{g}^-$. In addition, it is conditioned by the quality of the adaptive subtraction, which is not excellent. Moreover, we have only picked three primaries because of a priori knowledge, whereas without this information, strong artifacts in the adaptive subtraction could trick one into picking spurious reflectors. Nevertheless, in the ideal scenario where enough is known about the medium, either through further processing (preliminary velocity analy-

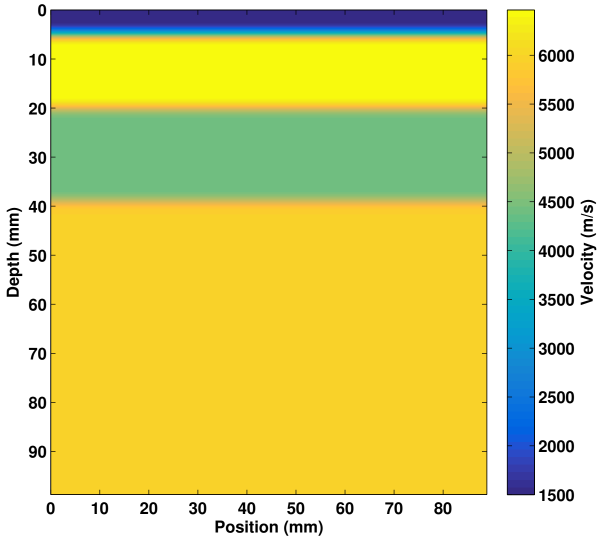


Figure 4: Velocity model used to compute adaptive Marchenko Green's functions and to perform migration. Zero depth corresponds to the surface of the array.

sis, S-wave removal, etc.) or a priori information, this method delivers high-quality images unaffected by spurious reflectors or adaptive-subtraction-related artifacts.

Despite the fact that one cannot obtain an exact Marchenko scaling using the $j$-curve analysis, a rough estimate based on convergence analysis may suffice (Ravasi et al., 2016). In this case, it is necessary to understand how the several Marchenko methods which require such scaling would perform under less-than-ideal conditions. This is an area which has so far been neglected, and which would be best served by testing under controlled laboratory conditions as has been done in this study.

## CONCLUSION

We presented an evaluation of three Marchenko-related methods using laboratory ultrasonic data. We show that estimating the scaling required for traditional Marchenko-based methods may be beyond current automated technology. We also present two adaptive Marchenko methods: the first an extension over a current adaptive Marchenko imaging method, and the second a primary construction method using adaptive Marchenko Green's functions as picking guides. The results show several improvements over RTM when using adaptive Marchenko methods, but less so than is expected from current literature. We thus demonstrate that laboratory experiments may help to understand and improve on current methods in the future.


## ACKNOWLEDGEMENTS

The authors thank the Edinburgh Interferometry Project sponsors (Schlumberger Cambridge Research, Statoil and Total) and the Wellcome Trust for supporting this research.


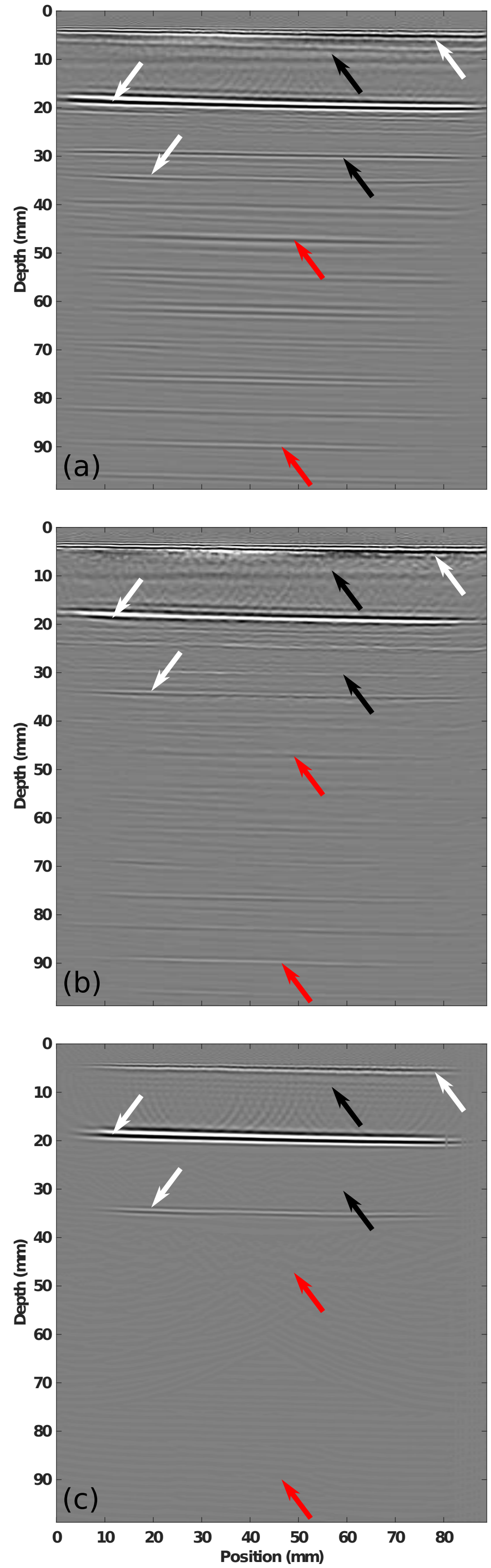


Figure 5: (a) RTM of processed dataset. (b) Adaptive Marchenko image. (c) Image of primaries-only dataset.

## REFERENCES


Amundsen, L., 2001, Elimination of free-surface related multiples without need of the source wavelet: Geophysics, **66**, 327–341.

Araújo, F. V., A. B. Weglein, P. M. Carvalho, and R. H. Stolt, 1994, Inverse scattering series for multiple attenuation: An example with surface and internal multiples: SEG Technical Program Expanded Abstracts 1994, 1039–1041.

Berkhout, A. J., and D. J. Verschuur, 2006, Imaging of multiple reflections: Geophysics, **71**, SI209–SI220.

Brackenhoff, J., 2016, Rescaling of incorrect source strength using Marchenko Redatuming: MSc Thesis, TU Delft.

Broggini, F., R. Snieder, and K. Wapenaar, 2012, Focusing the wavefield inside an unknown 1D medium: Beyond seismic interferometry: Geophysics, **77**, A25–A28.

Broggini, F., K. Wapenaar, J. van der Neut, and R. Snieder, 2014, Data-driven Green's function retrieval and application to imaging with multidimensional deconvolution: Journal of Geophysical Research: Solid Earth, **119**, 425–441.

Brown, M. P., and A. Guitton, 2005, Least-squares joint imaging of multiples and primaries: Geophysics, **70**, S79–S89.

da Costa Filho, C. A., G. A. Meles, and A. Curtis, 2017, Elastic internal multiple analysis and attenuation using Marchenko and interferometric methods: Geophysics, **82**, Q1–Q12.

da Costa Filho, C. A., M. Ravasi, and A. Curtis, 2015, Elastic P- and S-wave autofocus imaging with primaries and internal multiples: Geophysics, **80**, S187–S202.

Dokter, E., G. Meles, A. Curtis, and K. Wapenaar, 2017, Velocity analysis using surface-seismic primaries-only data obtained without removing multiples: Presented at the 79th EAGE Conference and Exhibition 2017.

Fleury, C., 2013, Increasing illumination and sensitivity of reverse-time migration with internal multiples: Geophysical Prospecting, **61**, 891–906.

Fokkema, J. T., R. G. van Borselen, and P. M. van den Berg, 1994, Removal of inhomogeneous internal multiples: Presented at the 56th EAGE Meeting and Technical Exhibition.

Fomel, S., 2009, Adaptive multiple subtraction using regularized nonstationary regression: Geophysics, **74**, V25–V33.

Jiang, Z., J. Yu, G. T. Schuster, and B. E. Hornby, 2005, Migration of multiples: The Leading Edge, **24**, 315–318.

Liu, Y., X. Chang, D. Jin, R. He, H. Sun, and Y. Zheng, 2011, Reverse time migration of multiples for subsalt imaging: Geophysics, **76**, WB209–WB216.

Malcolm, A. E., B. Ursin, and M. V. de Hoop, 2009, Seismic imaging and illumination with internal multiples: Geophysical Journal International, **176**, 847–864.

Meles, G. A., K. Löer, M. Ravasi, A. Curtis, and C. A. da Costa Filho, 2014, Internal multiple prediction and removal using Marchenko autofocusing and seismic interferometry: Geophysics, **80**, A7–A11.

Meles, G. A., K. Wapenaar, and A. Curtis, 2016, Reconstructing the primary reflections in seismic data by Marchenko redatuming and convolutional interferometry: Geophysics, **81**, Q15–Q26.

Mildner, C., T. S. Becker, K. de Vos, F. Broggini, and J. O. A. Robertsson, 2017, Source wavelet estimation using marchenko focusing functions: Theory and laboratory data example: Presented at the SEG Technical Program Expanded Abstracts 2017.

Ravasi, M., 2017, Rayleigh-Marchenko redatuming for target-oriented, true-amplitude imaging: Geophysics, **82**, S439–S452.

Ravasi, M., I. Vasconcelos, A. Kritski, A. Curtis, C. A. da Costa Filho, and G. A. Meles, 2016, Target-oriented Marchenko imaging of a North Sea field: Geophysical Journal International, **205**, 99–104.

Reiter, E. C., M. N. Toksöz, T. H. Keho, and G. M. Purdy, 1991, Imaging with deep-water multiples: Geophysics, **56**, 1081–1086.

Rose, J. H., 2001, "Single-sided" focusing of the time-dependent Schrödinger equation: Physical Review A, **65**, 0127071.

Singh, S., and R. Snieder, 2017, Source-receiver Marchenko redatuming: Obtaining virtual receivers and virtual sources in the subsurface: Geophysics, **82**, Q13–Q21.

Thomsen, H., 2016, Investigating the robustness of Green's function retrieval via Marchenko focusing and Seismic Interferometry: MSc Thesis, ETH Zürich.

van der Neut, J., J. Thorbecke, K. Wapenaar, and E. Slob, 2015a, Inversion of the Multidimensional Marchenko Equation: Presented at the 77th EAGE Conference and Exhibition 2015.

van der Neut, J., and K. Wapenaar, 2016, Adaptive overburden elimination with the multidimensional Marchenko equation: Geophysics, **81**, T265–T284.

van der Neut, J., K. Wapenaar, J. Thorbecke, and E. Slob, 2015b, Practical challenges in adaptive Marchenko imaging: SEG Technical Program Expanded Abstracts 2015, 4505–4509.

van der Neut, J., K. Wapenaar, J. Thorbecke, and I. Vasconcelos, 2014, Internal multiple suppression by adaptive Marchenko redatuming: SEG Technical Program Expanded Abstracts 2014, 4055–4059.

Vasconcelos, I., M. Ravasi, J. van der Neut, A. Kritski, and T. Cui, 2017, Retrieving Reservoir-Only Reflection and Transmission Responses From Target-Enclosing Extended Images: 79th EAGE Conference and Exhibition 2017, 12–15.

Verschuur, D. J., 1992, Adaptive surface-related multiple elimination: Geophysics, **57**, 1166.

Wapenaar, K., F. Broggini, E. Slob, and R. Snieder, 2013, Three-Dimensional Single-Sided Marchenko Inverse Scattering, Data-Driven Focusing, Green's Function Retrieval, and their Mutual Relations: Physical Review Letters, **110**, 0843011.

Wapenaar, K., J. Thorbecke, J. van der Neut, F. Broggini, E. Slob, and R. Snieder, 2014, Marchenko imaging: Geophysics, **79**, WA39–WA57.

Wapenaar, K., J. van der Neut, and E. Slob, 2016, Unified double- and single-sided homogeneous Green's function representations:

Proceedings of the Royal Society A: Mathematical, Physical and Engineering Science, **472**, 20160162.
Weglein, A. B., F. A. Gasparotto, P. M. Carvalho, and R. H. Stolt, 1997, An inverse-scattering series method for attenuating multiples in seismic reflection data: Geophysics, **62**, 1975–1989.
Youn, O. K., and H. Zhou, 2001, Depth imaging with multiples: Geophysics, **66**, 246–255.
Ziolkowski, A., D. B. Taylor, and R. G. K. Johnston, 1999, Marine seismic wavefield measurement to remove sea-surface multiples: Geophysical Prospecting, **47**, 841–870.
Zuberi, M. A. H., and T. Alkhalifah, 2014, Generalized internal multiple imaging (GIMI) using Feynman-like diagrams: Geophysical Journal International, **197**, 1582–1592.